Supporting Information

In situ pyrazolylborate ligand synthesis and coordination behaviours in aluminum oxo clusters

Jian-Bing Chen,[a,b] San-Tai Wang, [a,c] Si-Hao Shen, [a,c] Ying-Hua Yu, [a,c] Wei-Hui Fang,*[a] and Jian Zhang*[a]

[a] State Key Laboratory of Structural Chemistry, Fujian Institute of Research on the Structure of Matter, the Chinese Academy of Sciences, Fuzhou, Fujian 350002, People's Republic of China.

[b] School of Physical Science and Technology, ShanghaiTech University, Shanghai 201210 (P. R. China)

[c] *University of Chinese Academy of Sciences Chinese Academy of Sciences Beijing 100049, P. R. China.*

E-mail: fwh@fjirsm.ac.cn; zhj@fjirsm.ac.cn

Contents

Experimental Section

All the reagents and solvents were commercially and used as received without further purification. Aluminium isopropoxide, pyrazole and 4-methylpyrazole were acquired from Aladdin Chemical Reagent Shanghai. Phenylboronic acid, 3,5-bis(Trifluoromethyl)benzeneboronic, 3-chlorophenylboronic acid, 3-fluorophenylboronic acid, 4-fluorophenylboronic acid, ethanol (≥99.5%) and acetonitrile (≥ 99.5%) were acquired from Sinopharm Chemical Reagent Beijing.

Synthesis of AlOC-126 $[Al_2(L^1)_2(HL^1)_2 \cdot MeCN]$ (L^1=PhB(μ-O)$(pz)_2$)

A mixture of aluminium isopropoxide (204 mg, 1 mmol), phenylboronic acid (121 mg, 1 mmol), pyrazole (2 g, 29.38 mmol) and acetonitrile (2 mL) was sealed in a 20 mL vial and transferred to a preheated oven at 100 °C for 5 days. When cooled to room temperature, block colourless crystals were obtained. (yield: 42% based on $Al(O^iPr)_3$). The crystals are rinsed with ethanol and preserved under a sealed and dry environment. FT-IR (KBr, cm^{-1}): 1575(v), 1400(s), 1200(s), 1026(s), 769(s), 669(s), 495(s).

The synthesis of **AlOC-126-1** $[Al_2(L^{1'})_2(HL^{1'})_2 \cdot MeCN]$(($L^{1'}$=(3-F-PhB(μ-O)$(pz)_2$), **AlOC-126-2** $[Al_2(L^{1''})_2(HL^{1''})_2](L^{1''}$=(4-F-PhB(μ-O)$(pz)_2$), **AlOC-126-3** $[Al_2(L^{1'''})_2(HL^{1'''})_2]$ ($L^{1'''}$=(3-Cl-Ph(B(μ-O)$(pz)_2$) was replaced by different functionalized phenylboronic acids under the same synthesized conditions of **AlOC-126**.

Synthesis of AlOC-127 $[Al_4(L^2)_4(\mu_3\text{-}O)(pz\text{-}CH_3)_3) \cdot MeCN]$ (L^2=(3,5-Bis-CF_3-PhB(μ-O)$(pz\text{-}CH_3)_2$)

A mixture of aluminium isopropoxide (204 mg, 1 mmol), 3,5-bis(Trifluoromethyl) benzeneboronic acid, (257 mg, 1 mmol), 4-methylpyrazole (2 g, 24.36 mmol) and acetonitrile (2 mL) was sealed in a 20 mL vial and transferred to a preheated oven at 100 °C for 5 days. When cooled to room temperature, block colourless crystals were obtained. (yield: 21% based on $Al(O^iPr)_3$). The crystals are rinsed with ethanol and preserved under a sealed and dry environment. FT-IR (KBr, cm^{-1}): 3320(m), 2927(v), 2362(m), 1392(m), 1274(s), 1107(s), 850(s), 680(s).

Synthesis of AlOC-128 $[Al_6(L^3)_6(\mu_3\text{-}O)_2(pz\text{-}CH_3)_2]$ (L^3=(3-F-PhB(μ-O)$(pz\text{-}CH_3)_2$)

A mixture of aluminium isopropoxide (204 mg, 1 mmol), 3-fluorophenylboronic acid (139 mg, 1 mmol), 4-methylpyrazole (2 g, 24.36 mmol) and acetonitrile (2 mL) was sealed in a 20 mL vial and transferred to a preheated oven at 100 °C for 5 days. When cooled to room temperature, block colourless crystals were obtained. (yield: 38% based on $Al(O^iPr)_3$). The crystals are rinsed with ethanol and preserved under a sealed and dry environment. FT-IR (KBr, cm^{-1}): 2923(s), 2360(m), 1571(v), 1394(m), 1420(s), 1234(s), 1107(s), 774(s).

Z-scan measurements

The Z-scan technique[1] was applied to investigate the nonlinear optical (NLO) behavior of the samples with an output wavelength of 532 nm. A picosecond light source irradiated by a PL2250 laser (EKSPLA) was a Q-switched Nd: YAG pulsed laser system having a pulse width of 30 ps, a repetition frequency of 10 Hz, a beam waist radius of ω_0 of 23 μm, and a Rayleigh length of 3.12 mm. Liquid samples were measured in 2 mm quartz cuvettes for testing. The cuvettes were mounted on a computer-controlled translation stage that shifted the samples along the z axis and all test procedures were conducted at room temperature. For comparison, the linear transmittance of the sample was adjusted to be ~65%.

X-Ray crystallographic analysis

Crystallographic data of crystal **AlOC-126, AlOC-126-1, AlOC-126-2, AlOC-126-3, AlOC-127 and AlOC-128** were collected on Hybrid Pixel Array detector equipped with Ga-Kα radiation (λ = 1.3405 Å) at about 293 K. The structures were solved with the dual-direct methods using ShelXT and refined with the full-matrix least-squares technique based on F^2 with the SHELXL. Non-hydrogen atoms were refined anisotropically, while hydrogen atoms were added theoretically, riding on the concerned atoms and refined with fixed thermal factors. All absorption corrections were performed using the multi-scan program. The obtained crystallographic data are summarized in Table S1.

Table S1. Crystal data and structure refinement results (**AlOC-126**, **AlOC-126-1**, **AlOC-126-2**, **AlOC-126-3**, **AlOC-127**, **AlOC-128**)

Compound	**AlOC-126**	**AlOC-127**	**AlOC-128**
Formula	$C_{50}H_{49}Al_2B_4N_{17}O_4$	$C_{78}H_{61}Al_4B_4F_{24}N_{23}O_5$	$C_{92}H_{94}Al_6B_6F_6N_{28}O_8$
*M*r	1065.49	2055.71	2128.69
Temperature(K)	293 (2)	293 (2)	293 (2)
Wavelength (Å)	1.34050	1.34050	1.34050
Crystal system	triclinic	triclinic	monoclinic
Space group	*P-1*	*P-1*	*C2/c*
a/Å	11.9881(2)	14.79590(10)	18.8931(3)
b/Å	12.4767(2)	15.0054(2)	20.5399(3)
c/Å	21.5093(3)	22.6105(3)	27.5824(5)
α/°	100.2750(10)	81.1480(10)	90
β/°	97.0680(10)	82.3220(10)	91.246(2)
γ/°	117.664(2)	68.3070(10)	90
V/Å^3	2724.37(9)	4592.75(10)	10701.2(3)

Z	2	2	8
ρ/g cm^{-3}	1.299	1.536	1.321
μ/mm^{-1}	0.632	2.000	0.800
F(000)	1112.0	2064.0	4416.0
Collected reflns	39228	97698	39249
Unique reflns (R_{int})	12289(0.0327)	20483(0.0407)	11920(0.0504)
Completeness	1	1	1
GOF on F^2	1.093	1.033	1.082
R_1[a]/wR_2[b][$I > 2(I)$]	0.0430/0.1171	0.0807/0.2417	0.0596/0.1563
CCDC number	2234657	2234659	2234656

[a] $R_1 = \Sigma||F_o|-|F_c||/\Sigma|F_o|$ [b] $wR_2 = \{\Sigma[w(F_o^2-F_c^2)^2]/\Sigma[w(F_o^2)^2]\}^{1/2}$

Compound	**AlOC-126-1**	**AlOC-126-2**	**AlOC-126-3**
Formula	$C_{50}H_{45}Al_2B_4F_4N_{17}O_4$	$C_{48}H_{42}Al_2B_4F_4N_{16}O_4$	$C_{48}H_{42}Al_2B_4Cl_4N_{16}O_4$
*M*r	1119.21	1080.17	1144.97
Temperature(K)	293(2)	293(2)	293(2)
Wavelength (Å)	1.34050	1.34050	1.34050
Crystal system	triclinic	monoclinic	triclinic
Space group	*P-1*	*P2$_1$/c*	*P-1*
a/Å	12.1335(3)	16.8343(4)	11.7060(2)
b/Å	12.5287(3)	14.6616(3)	19.7341(3)
c/Å	21.5352(4)	21.2160(4)	24.0968(3)
α/°	97.791(2)	90	107.4400(10)
β/°	99.012(2)	92.643(2)	90.4670(10)
γ/°	118.010(3)	90	90.8220(10)
V/Å^3	2771.26(13)	5230.92(19)	5309.65(14)
Z	2	4	4
ρ/g cm^{-3}	1.341	1.372	1.432
μ/mm^{-1}	0.707	0.732	1.854
F(000)	1152.0	2224.0	2348.0
Collected reflns	26284	37476	66642
Unique reflns (R_{int})	9974(0.0201)	11474(0.0565)	23305(0.0699)
Completeness	0.99	0.98	0.99
GOF on F^2	1.062	1.068	1.061
R_1[a]/wR_2[b][$I > 2(I)$]	0.0424/0.1215	0.0692/0.1822	0.0879/0.2498
CCDC number	2234654	2234655	2234658

[a] $R_1 = \Sigma||F_o|-|F_c||/\Sigma|F_o|$ [b] $wR_2 = \{\Sigma[w(F_o^2-F_c^2)^2]/\Sigma[w(F_o^2)^2]\}^{1/2}$

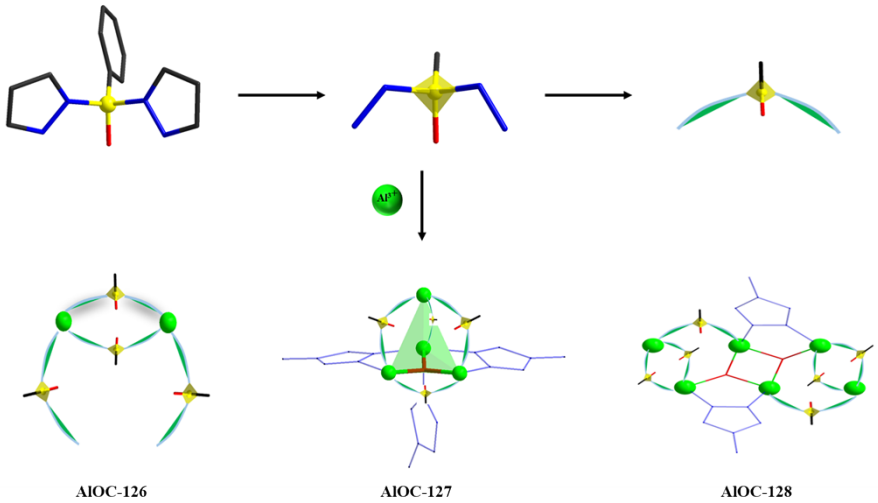

Fig. S1 Schematic diagram of the combination of L and Al^{3+} in the **AlOC-126, AlOC-127, AlOC-128.**

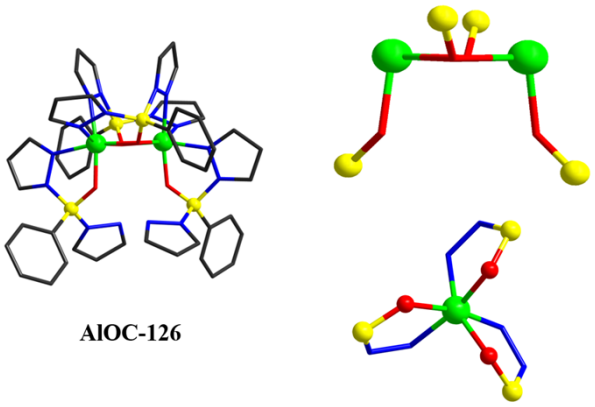

Fig. S2 Coordination environment of Al^{3+} ions and B-O-Al unit in **AlOC-126**. Color code: Al, green; C, black; O, red; N, blue; B, yellow.

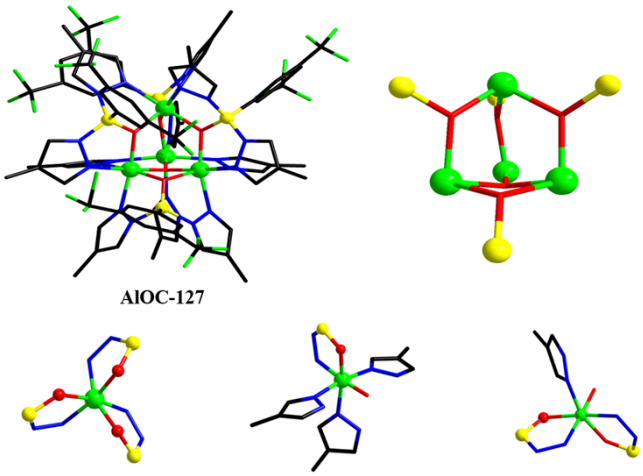

Fig. S3 Coordination environment of Al^{3+} ions and B-O-Al unit in **AlOC-127**. Color code: Al, green; C, black; O, red; N, blue; B, yellow; F, green.

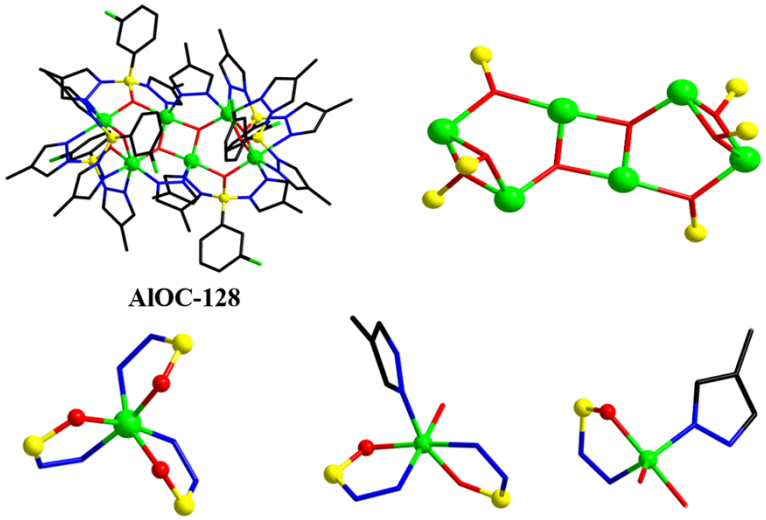

Fig. S4 Coordination environment of Al^{3+} ions and B-O-Al unit in **AlOC-128**. Color code: Al, green; C, black; O, red; N, blue; B, yellow; F, green.

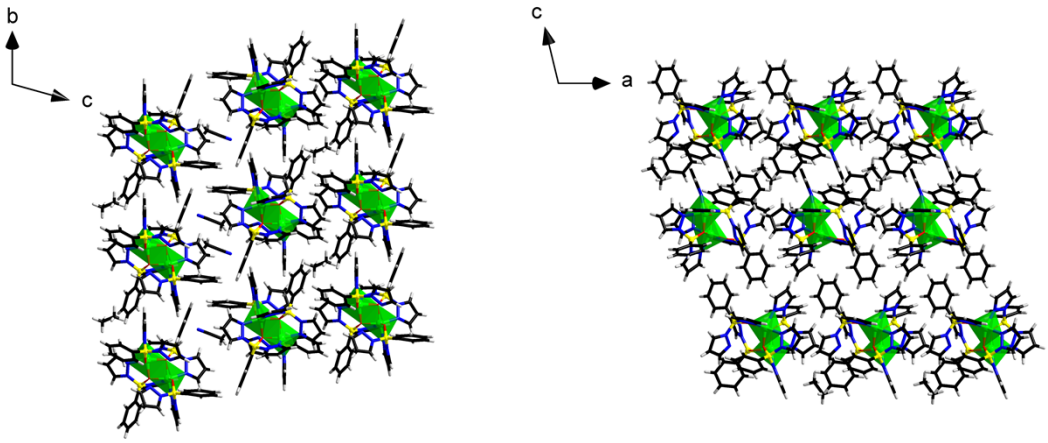

Figure S5. Packing diagrams of **AlOC-126** in the view of (a) a-axis and (b) c-axis.

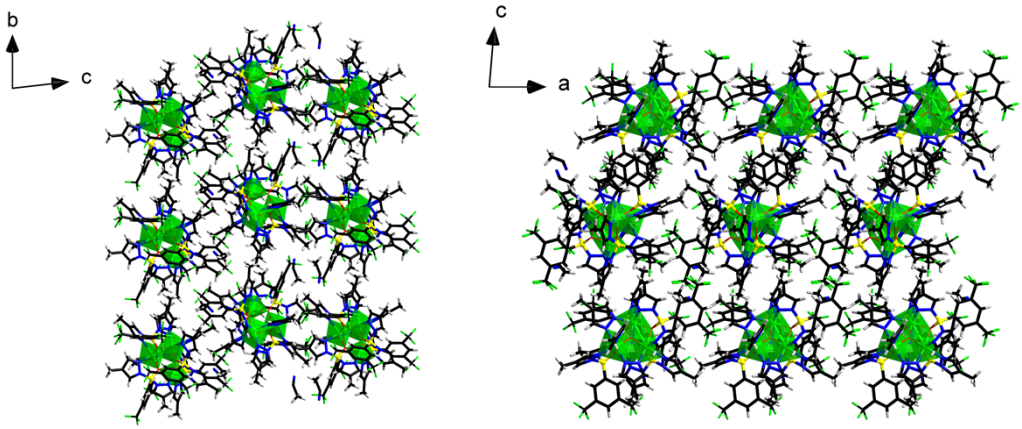

Figure S6. Packing diagrams of **AlOC-127** in the view of (a) a-axis and (b) c-axis.

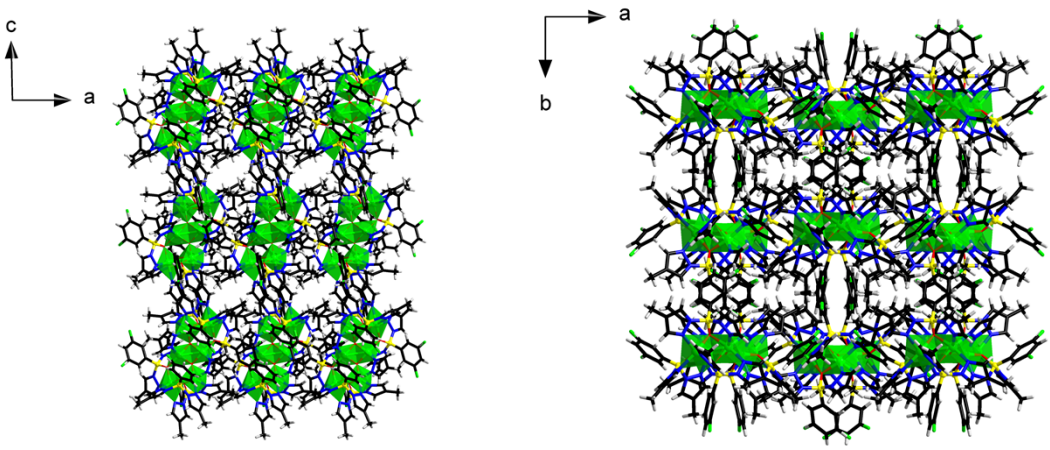

Figure S7. Packing diagrams of **AlOC-128** in the view of (b) a-axis and (c) c-axis.

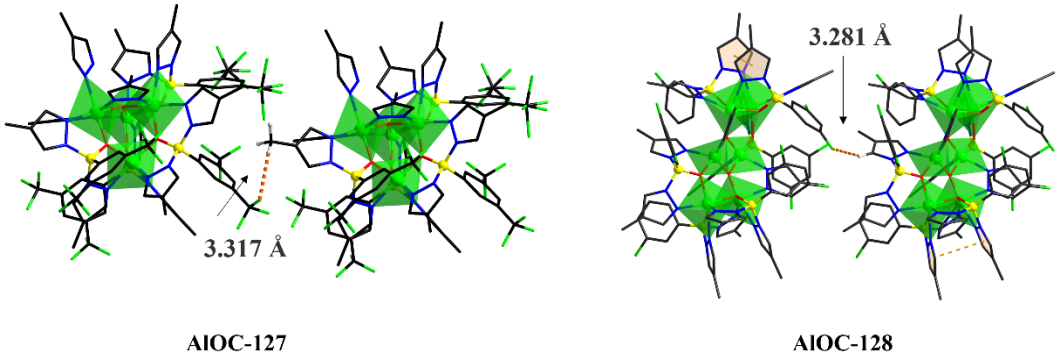

Figure S8. The hydrogen bond interactions (C-H···F) between F on benzene ring and C-H on 4-methylpyrazole in the **AlOC-127** and **AlOC-128**. Color code: Al, green; C, black; O, red; N, blue; B, yellow; F, green; H, white.

PXRD analyses for Al-O-B clusters

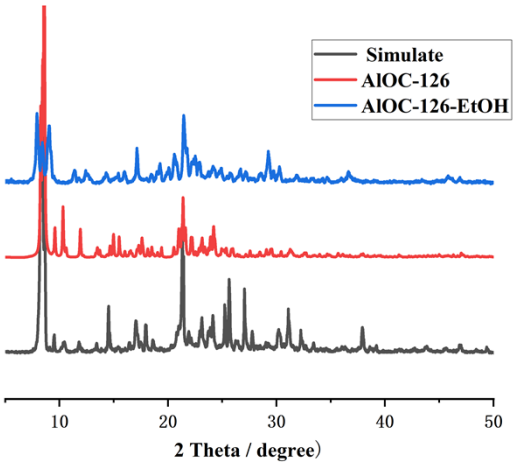

Figure S9. PXRD patterns of **AlOC-126**.

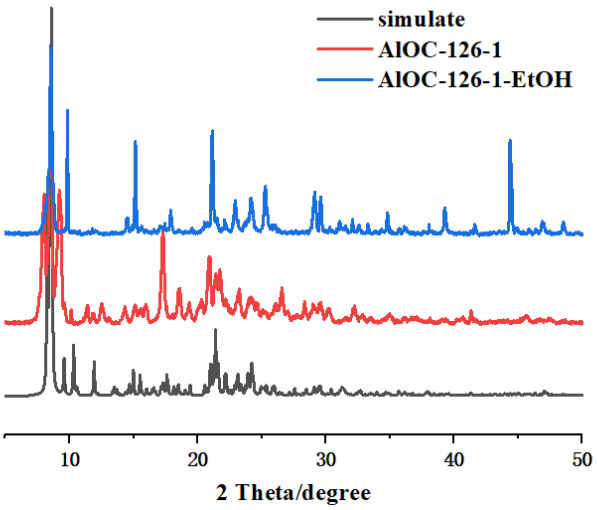

Figure S10. PXRD patterns of **AlOC-126-1**.

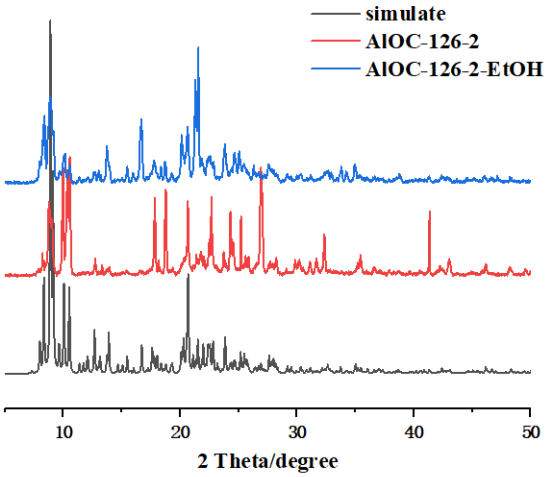

Figure S11. PXRD patterns of **AlOC-126-2**.

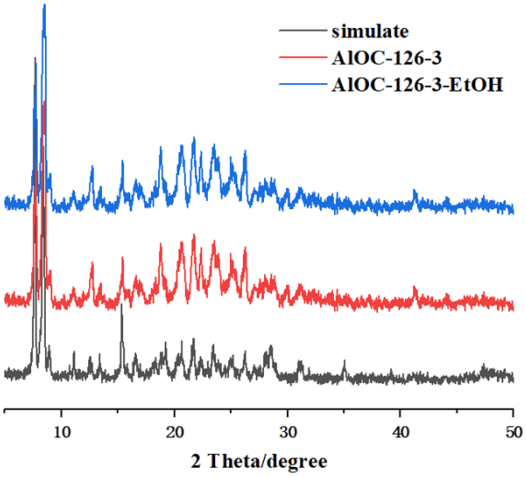

Figure S12. PXRD patterns of **AlOC-126-3**.

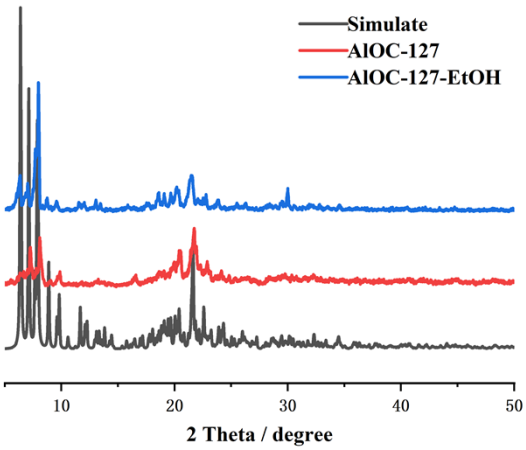

Figure S13. PXRD patterns of **AlOC-127.**

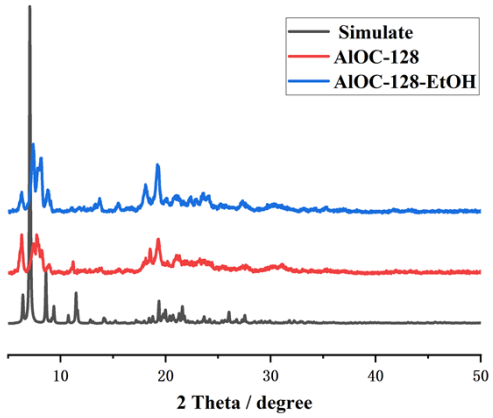

Figure S14. PXRD patterns of **AlOC-128.**

FT-IR spectra of Al-O-B clusters

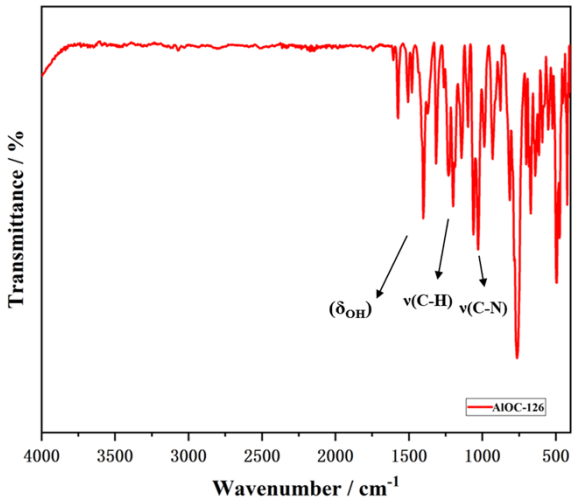

Figure S15. FT-IR spectra of **AlOC-126**.

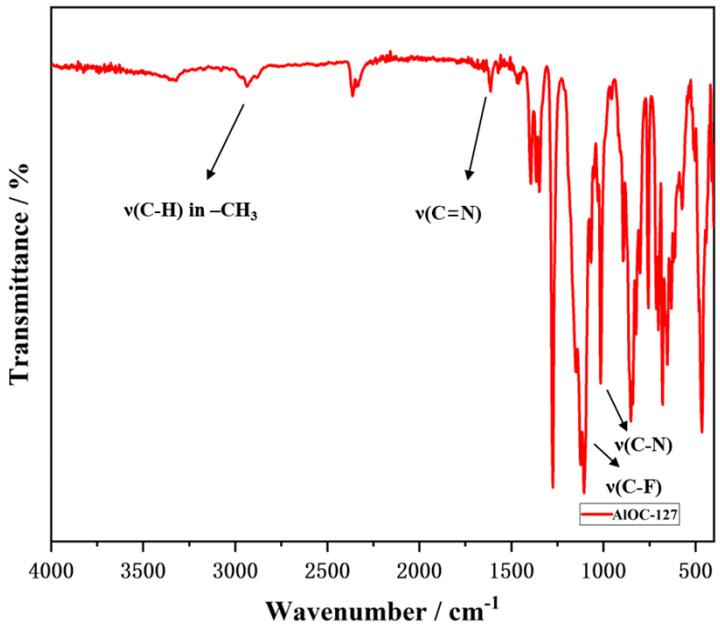

Figure S16. FT-IR spectra of **AlOC-127**.

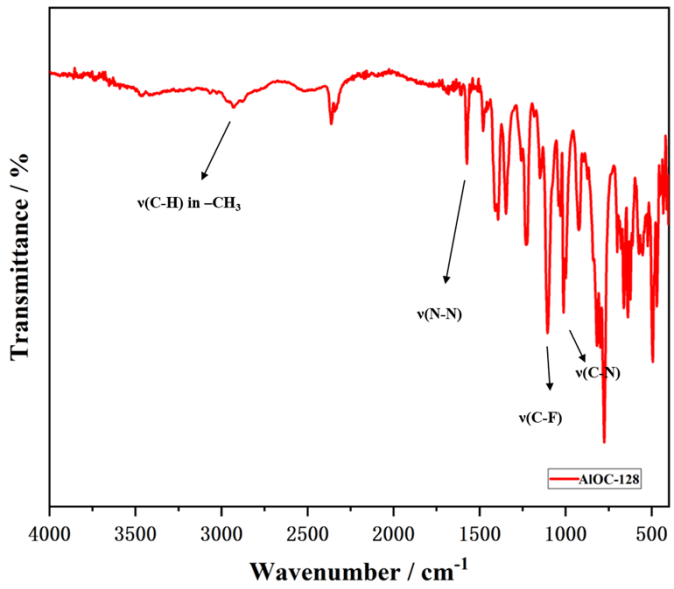

Figure S17. FT-IR spectra of **AlOC-128**.

It can be seen from the Fig. S15-S17 that **AlOC-126** has an δ_{OH} peak because of the incompletely protonated L exists in **AlOC-126**. Given that the introduction of functional groups F into the benzene ring and 4-methylpyrazole, **AlOC-127** and **AlOC-128** have $\nu_{(C-F)}$ and $\nu_{(C-H)}$ in $-CH_3$ peaks than **AlOC-126.**

EDS spectra of Al-O-B clusters

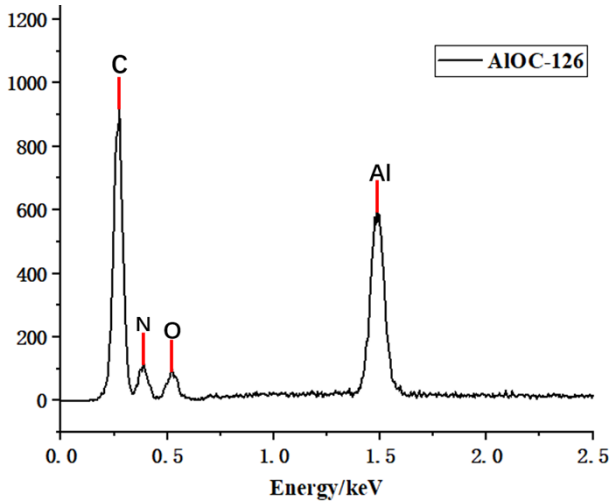

Figure S18. EDS spectra of **AlOC-126**.

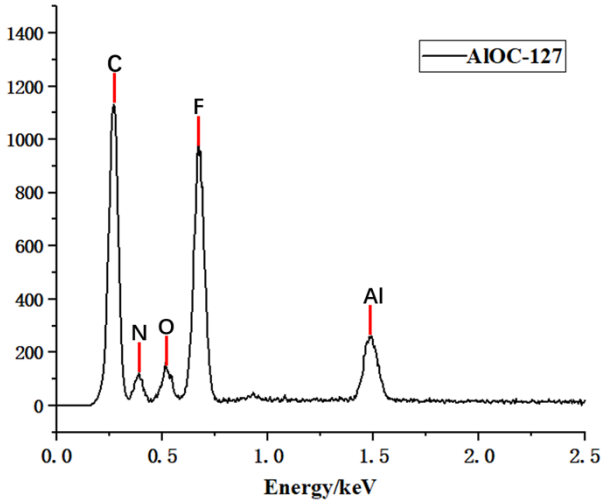

Figure S19. EDS spectra of **AlOC-127**.

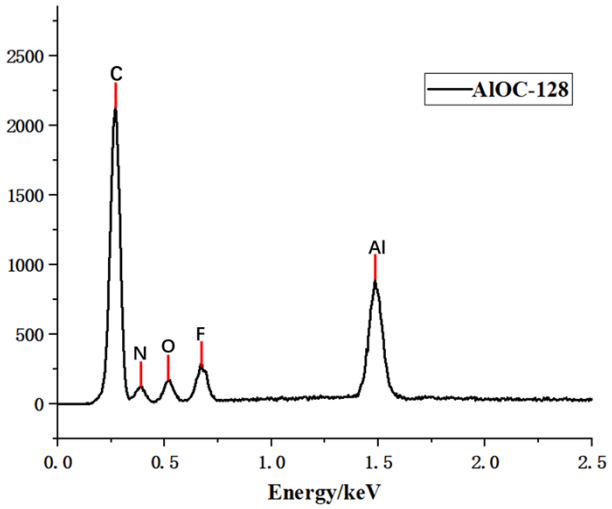

Figure S20. EDS spectra of **AlOC-128**.

The solid-state absorption spectra of Al-O-B clusters.

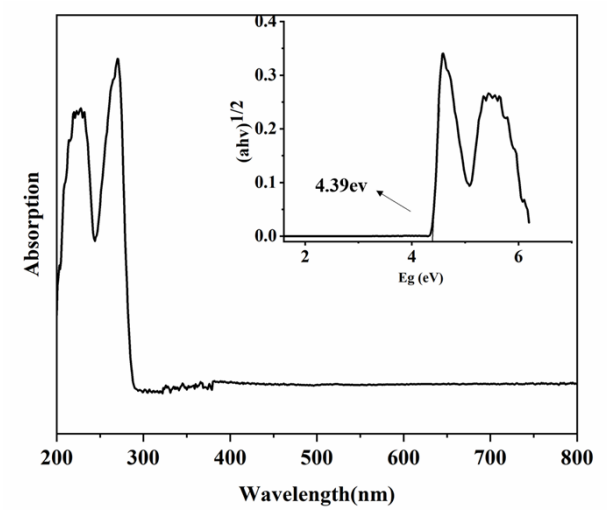

Figure S21. The solid-state absorption spectra of **AlOC-126**.

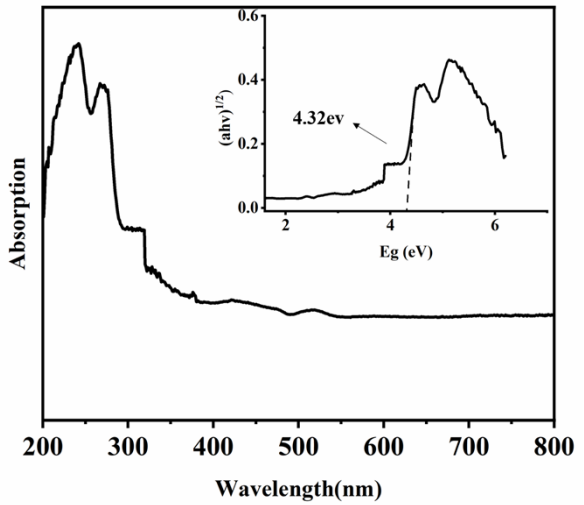

Figure S22. The solid-state absorption spectra of **AlOC-127**.

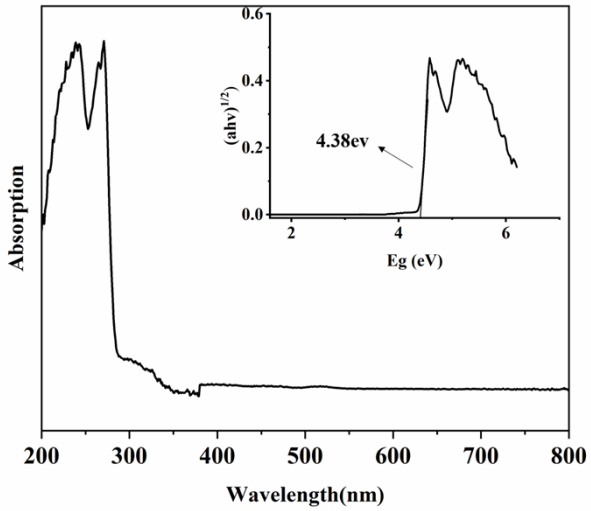

Figure S23. The solid-state absorption spectra of **AlOC-128**.

TGA spectra of Al-O-B clusters.

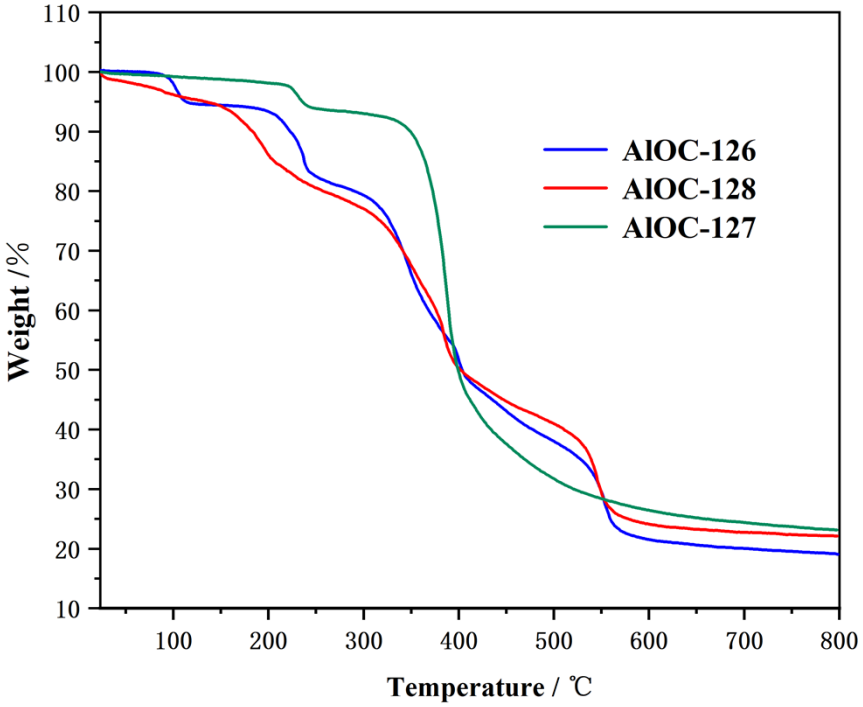

Figure S24. **TGA spectra of AlOC-126, AlOC-127, AlOC-128.**

The thermal stability of **AlOC-126** to **AlOC-128** was investigated in N_2 atmosphere up to 800 °C with a heating rate of 10 K min^{-1}, which is presented in Fig. S24. There are similar structures and compositions in AlOC-126 to AlOC-128, so only the TG investigation of **AlOC-12**7 was described in detail. **AlOC-127** with tetranuclear configuration can be stabilized at 217 °C before weight loss begins. It reveals a weight loss (6.7%) between 217 °C and 340 °C can be attributed to the removal of CH_3CN. The weight loss (64.5%) between 340 °C and 620 °C is assigned to the departure of the organic ligand owning to degradation of the structure.

Table S2. BVS analysis for **AlOC-126**.

Al01 3.328		**Al02 3.334**		**O004 1.316**		**O0AA 1.312**	
Al01-O003	1.8607	Al02-O003	1.8698	Al01-O004	1.8846	Al02-O0AA	1.8903
Al01-O004	1.8846	Al02-O005	1.8468	B01I- O004	1.461	B01Q-O0AA	1.459
Al01-O005	1.8825	Al02-O0AA	1.8903				
Al01-N007	1.9743	Al02-N00D	1.9699				
Al01-N009	1.9762	Al02-N00E	2.0762				
Al01-N00B	2.0570	Al02-N00L	1.9847				

Calculation of the nonlinear optical parameters

The following values are calculated and simulated according to the reported literature.[2, 3] The nonlinear absorption coefficient (β) can be determined by fitting Equation (1) with the experimental data obtained from the OA Z-scan. I_0: the on-axis peak intensity at the focus (Z = 0), L_{eff}: the effective thickness of the sample, α is the linear absorption coefficient, and l is the sample thickness; *n is the refractive index*; c: the speed of light; the imaginary part of the third-order nonlinear optical susceptibility $lm\chi^{(3)}$ was calculated from the relation that $lm\chi^{(3)}$ is in proportion to β; FOM could remove the discrepancy caused by the different linear absorption coefficient α. The relationship between the sample transmission and input laser intensity for a spatially Gaussian beam can be plotted from the open-aperture Z-scan curve. From the input laser pulse energy E_{in} and beam radius $\omega(z)$, the light fluence $F_{in}(z)$ at any position can be obtained.

$$T(Z, S=1) = \frac{1}{\pi^{-\frac{1}{2}}(Z,0)} \int_{-\infty}^{\infty} \ln\left[1 + q_0(Z,0)e^{-r^2}\right] dr \quad (1)$$

$$q_0(Z,0) = \beta I_0 L_{eff} \quad (2)$$

$$L_{eff} = \frac{1 - e^{-\alpha l}}{\alpha} \quad (3)$$

$$\omega(Z) = \frac{\omega_0}{\left[1 + \left(\frac{Z}{Z_0}\right)^2\right]^{-0.5}} \quad (4)$$

$$lm\chi^{(3)}(esu) = \left(\frac{10^{-7} n^2 \lambda c}{96\pi^2}\right)\beta \quad (5)$$

$$F_{in}(z) = \frac{4E_{in}\sqrt{ln2}}{\pi^{-\frac{3}{2}}\omega(z)^2} \quad (6)$$

$$FOM = \left|\frac{lm\chi^{(3)}}{\alpha}\right| \quad (7)$$

Table S3. Linear transmittance (T%), linear absorption coefficient (α), nonlinear absorption coeffificient (β), imaginary part of third-order nonlinear susceptibility ($\chi^{(3)}_I$), FOM, and T at 0.02 J/cm^2 of the AlOC-126, AlOC-127, AlOC-128.

samples	T (%)	A (cm^{-1})	β (cm/GW)	Im$\chi^{(3)}_I$ (×10^{-13}esu)	FOM	T at 0.02 J/cm^2 (%)
AlOC-126	65	4.31	0.41	1.60	1.93	72
AlOC-127	65	4.31	0.58	2.27	2.73	67
AlOC-128	65	4.31	0.87	3.40	4.09	52

References

1. C.-B. Yao, K.-X. Zhang and X. Wen, Focus introduction: Z-scan technique, *Optik*, 2017, **140**, 680-682.
2. Q.-F. Chen, X. Zhao, Q. Liu, J.-D. Jia, X.-T. Qiu, Y.-L. Song, D. J. Young, W.-H. Zhang and J.-P. Lang, Tungsten(VI)–Copper(I)–Sulfur Cluster-Supported Metal–Organic Frameworks Bridged by in Situ Click-Formed Tetrazolate Ligands, *Inorg. Chem.*, 2017, **56**, 5669-5679.
3. D.-J. Li, Q.-h. Li, Z.-R. Wang, Z.-Z. Ma, Z.-G. Gu and J. Zhang, Interpenetrated Metal-Porphyrinic Framework for Enhanced Nonlinear Optical Limiting, *J. Am. Chem. Soc.,* 2021, **143**, 17162-17169.